

Temperature dependence of the nitrogen-vacancy magnetic resonance in diamond

V. M. Acosta,^{1,*} E. Bauch,^{1,2} M. P. Ledbetter,¹ A. Waxman,³ L.-S. Bouchard,⁴ and D. Budker^{1,5,†}

¹ *Department of Physics, University of California, Berkeley, CA 94720-7300*

² *Technische Universität Berlin, Hardenbergstraße 28, 10623 Berlin, Germany*

³ *Department of Physics, Ben-Gurion University, Be'er-Sheva, 84105, Israel*

⁴ *Department of Chemistry and Biochemistry,*

University of California, Los Angeles, CA 90095

⁵ *Nuclear Science Division, Lawrence Berkeley National Laboratory, Berkeley CA 94720, USA*

(Dated: October 25, 2018)

The temperature dependence of the magnetic resonance spectra of nitrogen-vacancy (NV⁻) ensembles in the range of 280-330 K was studied. Four samples prepared under different conditions were analyzed with NV⁻ concentrations ranging from 10 ppb to 15 ppm. For all samples, the axial zero-field splitting (ZFS) parameter, D , was found to vary significantly with temperature, T , as $dD/dT = -74.2(7)$ kHz/K. The transverse ZFS parameter, E , was non-zero (between 4 and 11 MHz) in all samples, and exhibited a temperature dependence of $dE/(EdT) = -1.4(3) \times 10^{-4}$ K⁻¹. The results might be accounted for by considering local thermal expansion. The temperature dependence of the ZFS parameters presents a significant challenge for diamond magnetometers and may ultimately limit their bandwidth and sensitivity.

Magnetometers based on nitrogen-vacancy (NV) ensembles in diamond [1–3] promise high-sensitivity, rivaling those of superconducting quantum interference devices (SQUIDS) [4] and alkali vapor magnetometers [5], in a scaleable solid state system that can be operated over a wide range of temperatures. This remarkable combination of spatial resolution [6, 7] and magnetic sensitivity [8] make diamond magnetometers promising candidates for remote-detection and low-field nuclear magnetic resonance spectroscopy [9–12], nano-scale biological imaging [6, 13–15], and studies of novel magnetic and superconducting materials [3, 16]. Until now, the temperature dependence of the magnetic resonance spectra has not been systematically studied and has only briefly been mentioned in the literature [3, 17]. In this Letter, we report a striking temperature dependence of the magnetic-resonance spectra of NV⁻ ensembles in diamond over the temperature range of 280-330 K. These findings have important implications for the design of diamond magnetometers and may ultimately limit their sensitivity.

The resonance spectra were recorded using the continuous-wave Fluorescence Detected Magnetic Resonance (FDMR) method [17, 18]. Light from a 514-nm Argon-ion laser was focused with a 2.5 cm focal length lens onto the diamond samples, excit-

ing the NV⁻ centers' ${}^3A_2 \rightarrow {}^3E$ optical transition via a phonon sideband [19]. The same lens was used to collect fluorescence from the diamond which was then passed through a dichroic mirror and a 650-800 nm bandpass filter and detected with a photodiode. Noise due to laser power fluctuations was reduced by normalizing the fluorescence signal to a reference photodiode which monitored the incident laser power. The output of a microwave signal generator was amplified, passed through a straight $\sim 200\text{-}\mu\text{m}$ diameter copper wire of length ~ 5 mm placed within $500\ \mu\text{m}$ of the focused light beam, and terminated with $50\text{-}\Omega$ impedance. For temperature control, the diamond was thermally connected to a copper heatsink and placed inside an insulated aluminum housing. The temperatures of the heat sink and housing were controlled with separate thermoelectric (TE) elements. Unless otherwise stated, the results reported in this Letter were obtained with a magnetic field of $\lesssim 1$ G, laser-light power of ~ 150 mW, and microwave power (after the wire) of ~ 10 dBm.

For temperature scans, the temperature of the copper plate in direct thermal contact with the diamond was monitored with an AD590 sensor. The FDMR spectra were recorded with the temperature stabilized so that temperature excursions were less than 0.05 K over 5 min. In order to avoid stray magnetic fields when recording the spectrum, the currents supplied to both TE elements were chopped

*Electronic address: vmacosta@berkeley.edu

†Electronic address: budker@berkeley.edu

at a frequency of 2 Hz using photoMOS circuits, and the spectra were recorded only when the TE currents were off. The process was repeated until the temperature had been scanned through the 280-330 K range several times in both directions.

The NV-ensemble magnetic-resonance spectroscopy has been described, for example, in Refs. [2, 18, 20–22]) and is only briefly summarized here. Optical pumping via a spin-selective decay path collects NV centers (total spin $S = 1$) in the $|m_s = 0\rangle$ ground-state magnetic sublevel [19]. In the absence of external fields, the $|m_s = 0\rangle$ and $|m_s = \pm 1\rangle$ levels are split by an energy equal to the axial zero-field splitting (ZFS) parameter, $D \approx 2.87$ GHz. For perfect C_{3v} symmetry, the transverse ZFS parameter is $E = 0$ and the $|m_s = \pm 1\rangle$ levels remain degenerate. When the frequency of a microwave field that is transverse to the symmetry axis is tuned to the energy splitting between the $|m_s = 0\rangle$ and $|m_s = \pm 1\rangle$ levels, NV centers are transferred to the $|m_s = \pm 1\rangle$ sublevels, resulting in diminished fluorescence with a contrast as high as 30% [6]. In the presence of an applied magnetic field, B , the $|m_s = \pm 1\rangle$ levels split, revealing resonances separated by $2g_{NV}\mu_B B$, where $g_{NV} = 2.003$ is the NV⁻ Landé factor [20, 23] and μ_B is the Bohr magneton. For ensembles, there are four different NV orientations and, provided that $g_{NV}\mu_B|B| \ll D$, only the projection of the magnetic field on the N-V axis affects the transition frequencies [22].

The zero-field Hamiltonian for the ground state, including hyperfine coupling to the ^{14}N nucleus (spin $I = 1$), can be written as:

$$\begin{aligned} \mathcal{H}_0 \approx & DS_z^2 + E(S_x^2 - S_y^2) \\ & + A_{\parallel}S_zI_z + A_{\perp}(S_xI_x + S_yI_y), \end{aligned} \quad (1)$$

where $A_{\parallel} = -2.1$ MHz and $A_{\perp} = -2.7$ MHz are, respectively, the axial and transverse hyperfine constants [23]. Analysis of this Hamiltonian reveals six allowed microwave transitions for each N-V orientation. The relative intensities can be calculated by treating the interaction with the microwave field, \vec{B}_1 as a perturbation, $\mathcal{H}_1 = g_{NV}\mu_B\vec{B}_1 \cdot \vec{S}$, with matrix elements that depend on the alignment of the microwave radiation with respect to the symmetry and strain axes of each N-V center. However, since the exact geometry and the number of NV⁻ centers of each orientation were not known *a priori*, Gaussian functions with variable amplitudes and equal widths, centered about these transition frequencies,

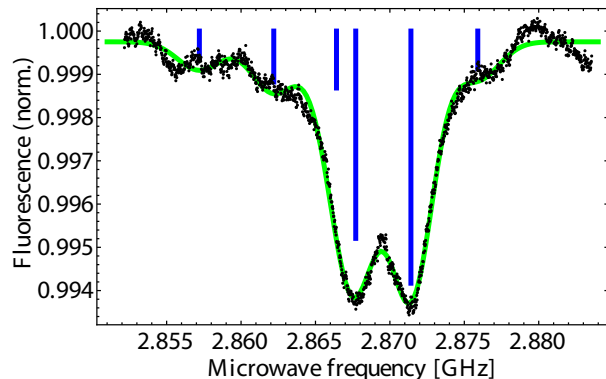


FIG. 1: Zero-field FDMR spectrum at 293 K for S3 and the corresponding fit based on Eq. 1 (solid green line). The six blue lines represent the fitted amplitudes at each transition frequency, and the fitted linewidth was 3.3 MHz (full width at half maximum). The microwave power was reduced to ~ -10 dBm to resolve the hyperfine structure, resulting in the relatively small contrast of $\sim 0.6\%$. The best-fit parameters for this scan are $E = 4.1(2)$ MHz and $D = 2866.8(2)$ MHz.

were fit to the spectra. Including residual magnetic fields, measured by a commercial fluxgate magnetometer to be less than 1 G, into the model did not significantly influence the fits.

Four single-crystal samples of mm-scale dimensions were studied, which were labeled S2, S3, S5, and S8 and characterized in Ref. [2]. Figure 1 shows the FDMR spectrum at 293 K for S3, a sample synthesized by chemical vapor deposition (CVD) with $[\text{NV}^-] \approx 10$ ppb [2]. As there was no applied magnetic field, the splitting between resonance peaks is due to non-zero E , induced by local strain [6, 22, 24]. This feature is present in varying magnitudes for all four samples. Even though all four NV orientations are present, the spectra are reasonably well-described by just six broad transitions, suggesting that the strain splittings are spatially inhomogeneous [17, 25]. As no correlation with NV⁻ concentration was observed (see Tab. I), further work is necessary to determine the exact strain mechanism.

During each temperature scan, the spectrum was fit to an empirical function similar to the one described above, and the ZFS parameters were extracted. Figure 2(a) displays the spectra at two different temperatures for another sample, S8, a high-pressure, high-temperature (HPHT) synthesized diamond with $[\text{NV}^-] \approx 0.3$ ppm, as well as the empirical fits based on Eq. 1. Figures 2(b) and (c) show the ZFS parameters as a function of temperature for

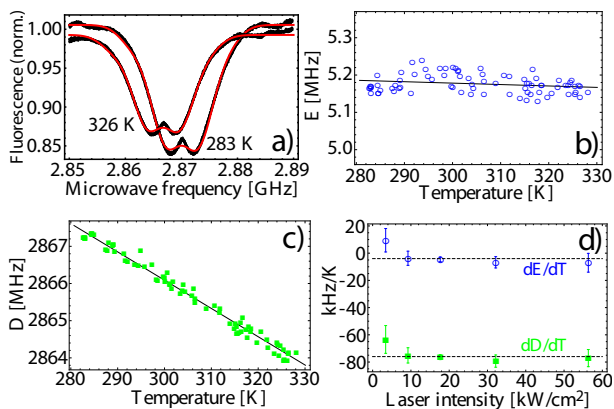


FIG. 2: (a) Zero-field FDMR spectra at 283 K and 326 K for S8 with fits (solid red lines). (b) Value of E for S8 as a function of temperature with linear fit (solid black line). (c) D for S8 vs. temperature with linear fit. (d) dD/dT and dE/dT as a function of laser intensity for S5. The dotted lines are the laser-intensity-independent values used in Tab. I.

this sample. Linear least-squares fits yield $dE/dT = -0.4(2)$ kHz/K and $dD/dT = -76(1)$ kHz/K. Figure 2(d) displays the laser-intensity dependence for S5, an HPHT diamond with $[NV^-] \approx 12$ ppm. Linear fits (not shown) determined that any dependence of dD/dT or dE/dT on laser intensity is not statistically significant. Additional tests for dependence on microwave power, external magnetic field, and sample positioning also did not show statistically significant effects.

A similar procedure was performed for the three other samples: S2, an HPHT diamond with $[NV^-] \approx 16$ ppm, as well as S3 and S5 (already mentioned). Table I displays the temperature dependence of the ZFS parameters for each of these samples. The temperature dependence of D is similar for each sample, indicating that the mechanism responsible for this temperature variation is intrinsic to the NV centers themselves. Taking a weighted average over all samples gives $dD/dT = -74.2(7)$ kHz/K and, using the fitted room-temperature values for each sample ($D \approx 2867(1)$ MHz), this corresponds to a fractional temperature dependence of $dD/(DdT) = -2.59(2) \times 10^{-5} \text{ K}^{-1}$. The weighted average over samples of the fractional variation of E with temperature (final column of Tab. I) is also statistically significant, $dE/(EdT) = -1.4(3) \times 10^{-4} \text{ K}^{-1}$, but further work is necessary to understand the nature of E .

The origin of D is expected to be predominately due to dipolar spin-spin coupling between the two

#	$[NV^-]$ (ppm)	$\frac{dD}{dT}$ (kHz/K)	E (MHz)	$\frac{1}{E} \frac{dE}{dT}$ (10^{-4}K^{-1})
S2	16	-71(1)	5.8(3)	-1.7(5)
S3	0.01	-79(2)	4.3(2)	2(5)
S5	12	-77(3)	11(1)	-3.6(9)
S8	0.3	-76(1)	5.2(1)	-0.8(4)

TABLE I: ZFS parameters and uncertainties for four different samples. The values of E represent the expected value of $E(293 \text{ K})$ extrapolated from the linear fits, and the error bars represent the standard error from the fit but not systematic effects due to imperfect assumptions in the model (see text). The laser intensity was $\sim 25\text{-}50 \text{ kW/cm}^2$ throughout the collection volume. Note that for the S2 spectra a magnetic field of $B_{\perp} \approx 13 \text{ G}$ was applied. This field enabled the isolation of a single NV orientation, and the simplified spectrum was used to verify the robustness of the model.

unpaired electrons forming the center [18, 20, 26]. This suggests a likely mechanism for the temperature variation is local lattice expansion. Assuming that the angular electronic wavefunctions are temperature-independent and that D is entirely due to dipolar coupling, the effect of lattice expansion on D is:

$$\frac{1}{D} \frac{dD}{dT} \approx \frac{1}{D} \frac{d\langle (r_{12}^2 - 3z_{12}^2)/r_{12}^5 \rangle}{dR} \frac{dR}{dT}, \quad (2)$$

where r_{12} is the displacement between the two spins, z_{12} is the component of r_{12} along the N-V symmetry axis, and R is the distance between two basal carbon nuclei. The effect of thermal expansion on $\langle (r_{12}^2 - 3z_{12}^2)/r_{12}^5 \rangle$ can be estimated by treating spins, localized near the basal carbon atoms [18, 27], with p -orbitals [18, 23] oriented along axes 110° apart [28], and calculating the integral for neighboring values of R . Using the room-temperature values for bulk diamond of $R = 0.252 \text{ nm}$ and $dR/dT = 2.52 \times 10^{-5} \text{ nm/K}$ [29], we calculate $D = 2.66 \text{ GHz}$, which is within 10% of the experimental value, and $dD/(DdT) = -5.8 \times 10^{-6} \text{ K}^{-1}$, which is about a factor of 4.5 smaller than the experimental value from this work. The latter discrepancy suggests that the macroscopic thermal expansion is not a good description of dR/dT in the immediate vicinity of the defect. *Ab initio* calculations [26–28, 30, 31] which include the determination of local thermal expansion effects would give a more accurate prediction of dD/dT .

The sharp temperature dependence of D presents a technical challenge for room-temperature diamond

magnetometry. Even if the ambient temperature can be controlled at the 1-mK level, this would lead to fluctuations in the resonance frequency of 80 Hz corresponding to a magnetic-field variation of 3 nT. Monitoring both of the $\Delta m_s = \pm 1$ resonances could provide a feedback mechanism for controlling this effect for slow drifts, since the energy difference between these resonances does not depend on D .

Higher-frequency temperature fluctuations due to, for example, laser-intensity noise, present an additional complication for magnetometry in the high-density limit. Consider the case of a Ramsey-type magnetometer making use of repeated light pulses [1, 6, 8, 15] which transfer an energy to the diamond on the order of $E_p \approx \Delta\epsilon[\text{NV}^-]V$, where $\Delta\epsilon \approx 0.6$ eV is the difference in energy between absorbed and radiated photons, V is the effective volume being heated, and we have conservatively neglected non-radiative transfer from the NV^- singlet decay path [32] and other impurities [33]. If the pulses are separated in time by a precession window, τ , then in steady state the diamond temperature is modulated at a rate $\frac{dT}{dt} \approx \frac{E_p}{Vc\tau}$, where $c = 1.8$ J/cm³/K is the volumetric specific heat of diamond [34]. Integration over the precession window yields a magnetometer offset of $B_{\text{off}} \approx \frac{\pi\Delta\epsilon[\text{NV}^-]}{g_{\text{NV}}\mu_{\text{BC}}} \frac{dD}{dT} \approx -80$ nT at room temperature for $[\text{NV}^-] = 1$ ppm. This offset makes the magne-

tometer sensitive to laser-pulse fluctuations. Uncorrelated, normally-distributed fluctuations in E_p by a fraction χ produce magnetic field noise-per-unit-bandwidth at the level of $\chi|B_{\text{off}}|/\sqrt{\tau} \approx 1$ pT/ $\sqrt{\text{Hz}}$, using $\chi = 0.01$ and $\tau = 1$ μs . We note that this magnetometer noise is directly correlated with laser-intensity noise and therefore monitoring the incident laser intensity could significantly reduce this effect.

In this work, we have measured the temperature dependence of the ZFS parameters of four diamond samples covering a wide range of NV^- concentrations. We have found a significant variation of the axial ZFS, D , with temperature and surmise that it is due to local thermal expansion. We also present evidence of a non-zero transverse ZFS, E , and measure a small fractional temperature dependence just above the experimental uncertainty. The results have a major impact on the performance of NV^- ensemble magnetometers and may ultimately limit their sensitivity and bandwidth. We expect that proper feedback mechanisms, such as monitoring laser intensity fluctuations and observing both $\Delta m_s = 1$ coherences simultaneously, will help to partially mitigate these effects.

The authors are grateful to A. Gali, C. Santori, P. Hemmer, F. Jelezko, E. Corsini, and O. Sushkov for valuable discussions and R. Folman for support. This work was supported by NSF grant PHY-0855552 and ONR-MURI.

-
- [1] J. M. Taylor, P. Cappellaro, L. Childress, L. Jiang, D. Budker, P. R. Hemmer, A. Yacoby, R. Walsworth, and M. D. Lukin, *Nat Phys* **4**, 810 (2008).
- [2] V. M. Acosta, E. Bauch, M. P. Ledbetter, C. Santori, K. M. C. Fu, P. E. Barclay, R. G. Beausoleil, H. Linget, J. F. Roch, F. Treussart, et al., *Physical Review B (Condensed Matter and Materials Physics)* **80**, 115202 (2009).
- [3] L. S. Bouchard, E. Bauch, V. M. Acosta, and D. Budker, *Detection of the meissner effect with a diamond magnetometer* (2009), arXiv:0911.2533v1 [cond-mat.supr-con].
- [4] J. Clarke and A. I. Braginski, *The SQUID Handbook*, vol. 1 (Wiley-VCH, Weinham, 2004).
- [5] D. Budker and M. Romalis, *Nature Physics* **3**, 227 (2007).
- [6] G. Balasubramanian, I. Y. Chan, R. Kolesov, M. Al-Hmoud, J. Tisler, C. Shin, C. Kim, A. Wojcik, P. R. Hemmer, A. Krueger, et al., *Nature* **455**, 648 (2008).
- [7] K. Y. Han, K. I. Willig, E. Rittweger, F. Jelezko, C. Eggeling, and S. W. Hell, *Nano Letters* **9**, 3323 (2009).
- [8] G. Balasubramanian, P. Neumann, D. Twitchen, M. Markham, R. Kolesov, N. Mizuochi, J. Isoya, J. Achard, J. Beck, J. Tissler, et al., *Nat Mater* **8**, 383 (2009).
- [9] S. K. Lee, M. Mossle, W. Myers, N. Kelso, A. H. Trabesinger, A. Pines, and J. Clarke, *Magnetic Resonance in Medicine* **53**, 9 (2005).
- [10] S. J. Xu, V. V. Yashchuk, M. H. Donaldson, S. M. Rochester, D. Budker, and A. Pines, *Proceedings of the National Academy of Sciences of the United States of America* **103**, 12668 (2006).
- [11] I. M. Savukov, S. J. Seltzer, and M. V. Romalis, *Journal of Magnetic Resonance* **185**, 214 (2007).
- [12] M. P. Ledbetter, I. M. Savukov, D. Budker, V. Shah, S. Knappe, J. Kitching, D. J. Michalak, S. Xu, and A. Pines, *Proceedings of the National*

- Academy of Sciences of the United States of America **105**, 2286 (2008).
- [13] D. Rugar, R. Budakian, H. J. Mamin, and B. W. Chui, *Nature* **430**, 329 (2004).
- [14] J. P. Cleuziou, W. Wernsdorfer, V. Bouchiat, T. Ondarcuhu, and M. Monthieux, *Nat Nano* **1**, 53 (2006).
- [15] J. R. Maze, P. L. Stanwix, J. S. Hodges, S. Hong, J. M. Taylor, P. Cappellaro, L. Jiang, M. V. G. Dutt, E. Togan, A. S. Zibrov, et al., *Nature* **455**, 644 (2008).
- [16] J. R. Kirtley, A. C. Mota, M. Sigrist, and T. M. Rice, *Journal of Physics-Condensed Matter* **10**, L97 (1998).
- [17] A. Gruber, A. Drabenstedt, C. Tietz, L. Fleury, J. Wrachtrup, and C. von Borczyskowski, *Science* **276**, 2012 (1997).
- [18] X. F. He, N. B. Manson, and P. T. H. Fisk, *Physical Review B* **47**, 8816 (1993).
- [19] N. B. Manson, J. P. Harrison, and M. J. Sellars, *Physical Review B* **74** (2006).
- [20] J. Loubser and J. A. van Wyk, *Reports on Progress in Physics* **41**, 1201 (1978).
- [21] T. P. M. Alegre, C. Santori, G. Medeiros-Ribeiro, and R. G. Beausoleil, *Physical Review B (Condensed Matter and Materials Physics)* **76**, 165205 (2007).
- [22] N. D. Lai, D. Zheng, F. Jelezko, F. Treussart, and J.-F. Roch, *Applied Physics Letters* **95**, 133101 (2009).
- [23] S. Felton, A. M. Edmonds, M. E. Newton, P. M. Martineau, D. Fisher, D. J. Twitchen, and J. M. Baker, *Physical Review B (Condensed Matter and Materials Physics)* **79**, 075203 (2009).
- [24] G. D. Fuchs, V. V. Dobrovitski, R. Hanson, A. Batura, C. D. Weis, T. Schenkel, and D. D. Awschalom, *Physical Review Letters* **101**, 117601 (2008).
- [25] A. P. Nizovtsev, S. Y. Kilin, C. Tietz, F. Jelezko, and J. Wrachtrup, *Physica B: Condensed Matter* **308-310**, 608 (2001).
- [26] A. Lenef and S. C. Rand, *Physical Review B* **53**, 13441 (1996).
- [27] A. Gali, M. Fyta, and E. Kaxiras, *Physical Review B* **77** (2008).
- [28] J. P. Goss, R. Jones, S. J. Breuer, P. R. Briddon, and S. Oberg, *Physical Review Letters* **77**, 3041 (1996).
- [29] T. Sato, K. Ohashi, T. Sudoh, K. Haruna, and H. Maeta, *Physical Review B* **65**, 092102 (2002).
- [30] M. Luszczek, R. Laskowski, and P. Horodecki, *Physica B-Condensed Matter* **348**, 292 (2004).
- [31] A. Gali, E. Janzen, P. Deak, G. Kresse, and E. Kaxiras, *Physical Review Letters* **103**, 186404 (2009).
- [32] L. G. Rogers, S. Armstrong, M. J. Sellars, and N. B. Manson, *New Journal of Physics* **10**, 103024 (2008).
- [33] G. Davies and M. Crossfield, *Journal of Physics C-Solid State Physics* **6**, L104 (1973).
- [34] A. C. Victor, *The Journal of Chemical Physics* **36**, 1903 (1962).